

## Strut-tie model evaluation of behavior and strength of pre-tensioned concrete deep beams

Young Mook Yun

*Department of Civil Engineering, Kyungpook National University, Daegu 702-701, Korea*

(Received June 19, 2004, Accepted August 10, 2005)

**Abstract.** To date, many studies have been conducted for the analysis and design of reinforced concrete members with disturbed regions. However, prestressed concrete deep beams have not been the subject of many investigations. This paper presents an evaluation of the behavior and strength of three pre-tensioned concrete deep beams failed by shear and bond slip of prestressing strands using a nonlinear strut-tie model approach. In this approach, effective prestressing forces represented by equivalent external loads are gradually introduced along strand's transfer length in the nearest strut-tie model joints, the friction at the interface of main diagonal shear cracks is modeled by the aggregate interlock struts along the direction of the cracks in strut-tie model, and an algorithm considering the effect of bond slip of prestressing strands in the strut-tie model analysis and design of pre-tensioned concrete members is implemented. Through the strut-tie model analysis of pre-tensioned concrete deep beams, the nonlinear strut-tie model approach proved to present effective solutions for predicting the essential aspects of the behavior and strength of pre-tensioned concrete deep beams. The nonlinear strut-tie model approach is capable of predicting the strength and failure modes of pre-tensioned concrete deep beams including the anchorage failure of prestressing strands and, accordingly, can be employed in the practical and precise design of pre-tensioned concrete deep beams.

**Keywords:** pre-tensioned concrete deep beam; nonlinear strut-tie model approach; behavior and strength; gradual introduction of prestressing force; aggregate interlock strut; bond slip of prestressing strand.

### 1. Introduction

Concrete members behave nonlinearly according to the loading and boundary conditions, material properties, interactions between concrete and reinforcement, concrete cracks, etc. Particularly, in the case of pre-tensioned concrete deep beams in which the prestressing forces by prestressing strands are transferred to concrete by bond the redistribution of internal forces occurs before failure, and their load transfer mechanism is greatly different from that of usual beams. Therefore, it is necessary to employ strut-tie models for the rational design and precise behavior and strength evaluation of pre-tensioned concrete deep beams.

Until now, the strut-tie model analyses and designs have been adapted mainly to reinforced concrete members with disturbed stress regions such as reinforced concrete deep beams, dapped beams, corbels, post-tensioned concrete anchorage zones, etc. (Chen, *et al.* 1987, Schlaich, *et al.* 1987, Siao 1993, 1994, Foster, *et al.* 1996, Sanders and Breen 1997, Maxwell and Breen 2000,

---

† Associate Professor, E-mail: [ymyun@knu.ac.kr](mailto:ymyun@knu.ac.kr)

Foster and Malik 2002, Yun 2005). However, there have not been many investigations dealing with the analysis and design of pre-tensioned concrete deep beams (Alshegeir and Ramirez 1992, Tan, *et al.* 2001). The current study evaluates the behavior and strength of three types of pre-tensioned concrete deep beams tested to failure using the nonlinear strut-tie model approach (Yun 2000) and a computer graphic program NL-STM (Yun 2000) designed for practical use of strut-tie model analysis and design. An algorithm that considers the bond slip behavior of pre-tensioned concrete deep beams is developed and implemented into the nonlinear strut-tie model approach. Based on the results of the current study, the validity of the nonlinear strut-tie model approach in the nonlinear analysis of pre-tensioned concrete deep beams is discussed. In addition, the effects of the gradual introduction of prestressing force to a selected strut-tie model, the friction at the interfaces of shear cracks, and the bond slip of prestressing strands on the behavior and strength of the pre-tensioned deep beams are investigated.

## 2. Nonlinear strut-tie model approach

Selecting a strut-tie model in the nonlinear strut-tie model approach is an iterative process. In this process, the first step is to select the initial truss model. The next step is to calculate the effective strengths, cross-sectional areas, and the member forces of struts and ties. The last step is to examine the conditions of geometric compatibility and nodal zone strength of the strut-tie model. If the cross-sectional areas of two almost parallel concrete struts placed side by side overlap with each other or the dimensioned strut-tie model is not compatible with the actual size of the structural concrete, the strut-tie model itself and/or its geometry must be modified and the procedure repeated until a satisfactory solution is obtained.

The nonlinear strut-tie model approach for reinforced concrete members incorporates nonlinear techniques in the selection, analysis, and verification processes of a strut-tie model to eliminate the limitations of the conventional strut-tie model approaches relating to the behavior and strength predictions of structural concrete and the design of structural concrete which experiences nonlinear behavior. The approach also incorporates additional positioning of concrete ties at the locations of steel ties. The nonlinear strut-tie model approach for pre-tensioned concrete members also incorporates the same nonlinear techniques and additional positioning of concrete ties with those for reinforced concrete members. However, unlike the approach for reinforced concrete members, the approach for pre-tensioned concrete members incorporates the effects of the gradual introduction of prestressing forces on a selected strut-tie model, the aggregate interlock action at the interfaces of shear cracks, and the bond slip behavior of prestressing strands in the strut-tie model analysis and design.

### 2.1. Transfer of prestressing force

In prestressed concrete, the prestressing force is usually transferred to the concrete by bond and anchorage devices. When prestressing strands are pre-tensioned, their stress is often transferred to the concrete solely by bond between the two materials. Thus, there is a length of transfer at each end of strands that performs the function of anchorage, when mechanical end anchorages are not provided. At anchorage, bond stress exists immediately after transfer. The stress in the strands varies from zero at the exposed end to a full prestresss at some distance inside the concrete. The distance is known as the transfer length, and the distance that a prestressing strand requires to reach ultimate

strength is known as the development length. The development length of a prestressing strand,  $L_d(\text{mm})$ , is described by AASHTO-LRFD (1998) as follows:

$$L_d \geq 0.048f_{se}d_b + 0.145(f_{ps} - f_{se})d_b \quad (1)$$

where,  $d_b(\text{mm})$ ,  $f_{ps}(\text{MPa})$ , and  $f_{se}(\text{MPa})$  are the cross section diameter of the prestressing strand, the ultimate strength of the strand, and the effective prestress of the strand, respectively. The first term of Eq. (1),  $0.048f_{se}d_b$ , is the transfer length that is necessary to deliver the effective prestress of the strand to the concrete.

Prestressing force generates compressive force to concrete and tensile to the prestressing strand. The direction of the prestressing force is different, but its magnitude is the same. The prestressing force affects both the load path and the stress caused by the external load in the service and ultimate load conditions. Thus, how to apply the prestressing force is important in strut-tie model analysis and design of pre-tensioned concrete members. Schlaich, *et al.* (1987) suggested that to account for the prestressing force effect, prestressing force must be applied as a permanent load which does not change after clearing the prestressing jack. Alshegeir and Ramirez (1992) adapted Schlaich's model by considering the prestressing force not as initial prestressing force, but as effective prestressing force. Accordingly, the current study deals with their suggestions, and applies the prestressing force to a strut-tie model by considering development length. Assuming that the prestressing force in a pre-tensioned concrete member is introduced to concrete linearly bond, the effective prestressing force is applied to the strut-tie model nodes within the transfer length through linear interpolation, as is shown in Fig. 1.

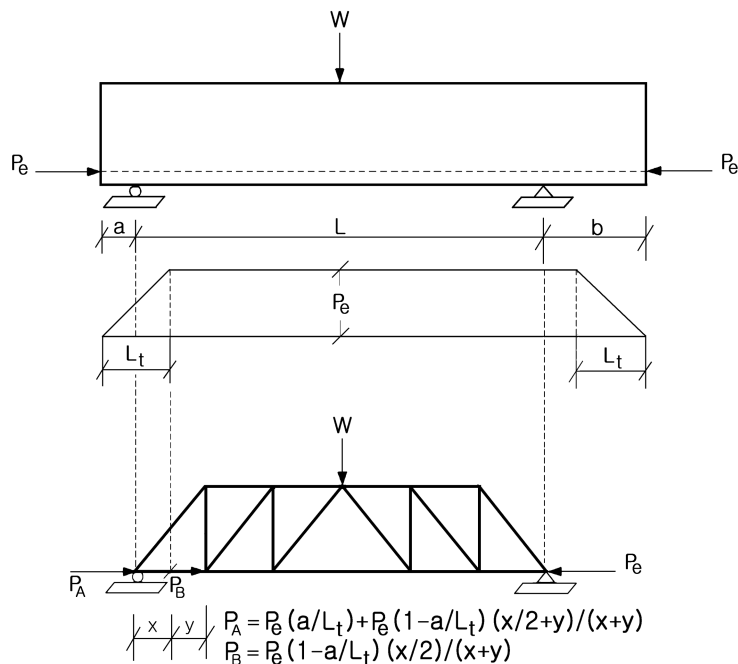


Fig. 1 Prestressing force in pre-tensioned member with fully bonded strands

## 2.2. Effect of shear friction

In a prestressed concrete beam, the initial prestressing force of a strand enhances the resistance force by compressing the concrete against a large external load before cracking. After cracking, the prestressing force of a strand limits the width of crack. Thus, it causes friction force in concrete cracks. Fig. 2 shows the shear resistance in cracked sections. When reinforcing bars and the cracked section meet vertically, the shear resistance force is expressed as Eq. (2), and when they meet slantly, it is expressed as Eq. (3):

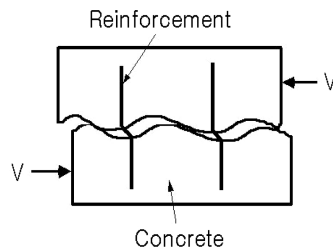
$$V_n = \mu A_{vf} f_y \quad (2)$$

$$V_n = \mu A_{vf} f_y \cos \theta + A_{vf} f_y \sin \theta \quad (3)$$

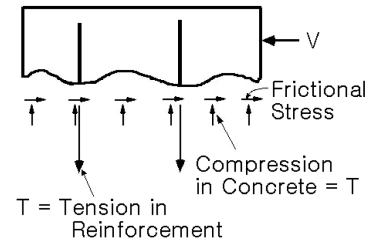
where,  $\mu (=0.8)$  is the friction coefficient of a cracked section,  $A_{vf}$  is the cross section area of shear reinforcing bars in a cracked section,  $f_y$  is the tensile strength of shear reinforcing bars, and  $\theta$  is the inclination angle of a crack.

In the current study, the friction force in shear cracks is considered by adding a diagonal strut (shear friction strut) connected to the vertical load point to supports. The stiffness of the shear friction strut,  $AE$ , is determined when the strut force in left side of Eq. (4) obtained from the analysis of a selected strut-tie model is the same as the friction force in right side of Eq. (4) obtained using the vertical steel tie forces of a selected strut-tie model,  $\Sigma F_{tie}$ :

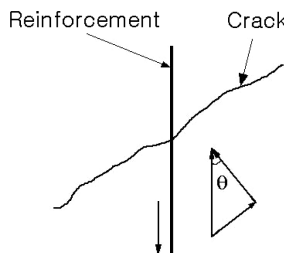
$$F = \mu \Sigma F_{tie} \cdot \cos \theta \quad (4)$$



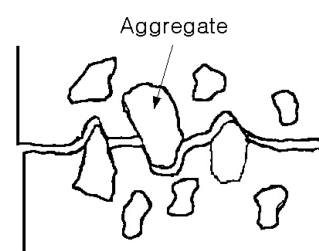
(a) Shear Friction causing Crack



(b) Free-body Diagram



(c) Shear Friction Reinforcement



(d) Aggregate Interlock at Crack

Fig. 2 Shear friction concept

where  $F_{tie} (= A_{vf} f_s \leq A_{vf} f_y)$ ,  $f_s$  = tensile stress of a vertical steel tie) is the vertical steel tie force of a selected strut-tie model and  $\theta$  is the inclination angle of the shear friction strut.

### 2.3. Effect of bond slip

In the analysis and design of concrete members it is assumed that reinforcement and concrete are completely bonded, and that they then behave as one body. However, the assumption is effective only for concrete members in which bond stress occurring between the reinforcement and concrete can be ignored. In the contact surface of the reinforcement and concrete in a cracked region, significant bond stress related to relative displacement of reinforcement and concrete occurs. Reinforcements and concrete around cracks show differences in strain, which is called bond slip. Bond slip is possible only when the bond stress occurring by the difference  $\Delta T (= T_2 - T_1)$  of tensile force  $T_1$  and  $T_2$  acting on two random sections in Fig. 3, is larger than the average bond stress. Although various average bond stresses have been proposed by various experiments and analytical methods, the current study used the average bond stress equation derived by a theoretical method (Eq. (5), Mac Gregor 1997) to evaluate the behavior and strength of pre-tensioned concrete members in which bond slips have occurred.

In the current study, an algorithm that evaluates the behavior and strength of concrete members in which bond slips occur is incorporated with the nonlinear strut-tie model approach. The flowchart for the algorithm is shown in Fig. 4. In the algorithm, the occurrence of bond slip in a steel tie,  $i$ , is judged by comparing the average bond stress of the steel tie,  $\mu_{avg,i}$ , obtained from Eq. (5), and the bond stress of the steel tie,  $\mu_i$ , obtained from Eq. (6).

$$\mu_{avg} = 6\sqrt{f_c'} \left( \frac{c}{d_b} - \frac{1}{2} \right) \quad (5)$$

$$\mu = \frac{\Delta T}{\Delta x \pi d_b} \quad (6)$$

in which  $f_{ct}$  is the tensile strength of concrete,  $d_b$  is the diameter of reinforcing bar,  $c$  is the smaller of the smallest distance measured from the center of reinforcing bar to the surface of concrete member, or one-half of center-to-center spacing of reinforcing bars ( $y$  and  $z$  values in Fig. 5), and  $\Delta x$  is the length of reinforcement, i.e., the length of a steel tie in a strut-tie model. In addition,  $\Delta T_i$  in Eq. (6) is the difference of cross-sectional forces between steel ties, which can be written as follows:

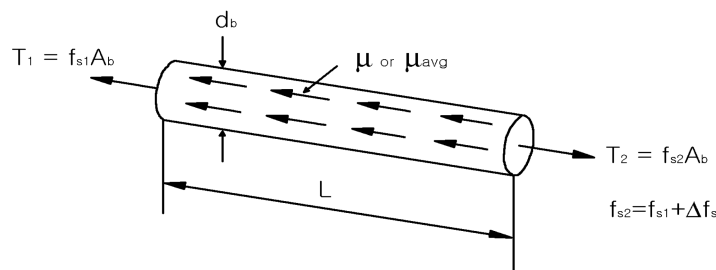


Fig. 3 Bond stresses in reinforcement steel

$$\Delta T_i = \frac{x_i}{x_{i+1} + x_i} (T_{i+1} - T_i) + \frac{x_i}{x_{i-1} + x_i} (T_i - T_{i-1}) \quad (7)$$

in which  $x_{i-1}$  and  $x_{i+1}$  are the lengths of steel ties  $i-1$  and  $i+1$  located at the left and right side

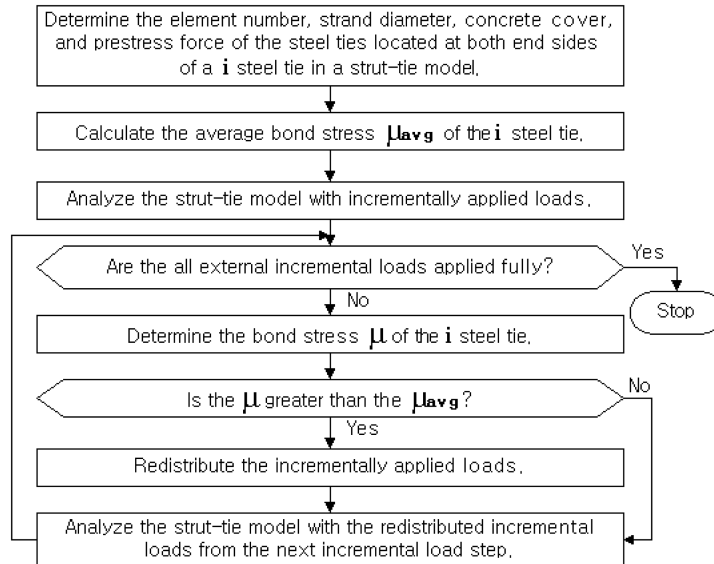


Fig. 4 Algorithm for considering bond slip behavior in nonlinear strut-tie model approach

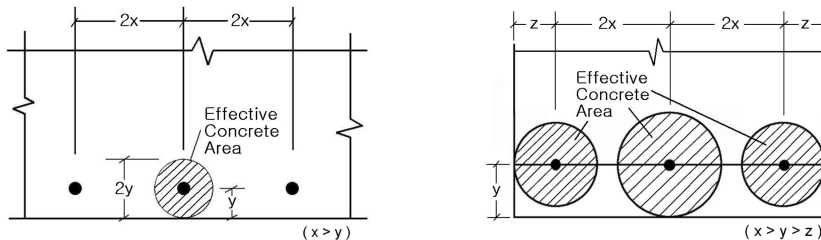


Fig. 5 Effective cross-sectional area of concrete tie

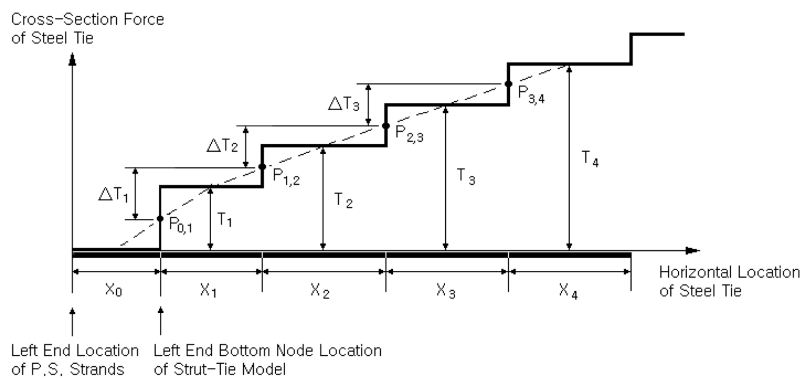


Fig. 6 Graphical description of member force difference  $\Delta T$

of steel tie  $i$ , respectively, and  $T_{i-1}$  and  $T_{i+1}$  are the member forces of steel ties  $i-1$  and  $i+1$ , respectively. The value  $\Delta T_i$  in Eq. (7), as shown in Fig. 6, is one-half of the difference of the value between  $P_{i-1,i}$ , a point intersected by a straight line connecting the member forces of steel ties  $i-1$  and  $i$  in their middle points in length, and  $P_{i,i+1}$ , a point intersected by a straight line connecting the member forces of steel ties  $i$  and  $i+1$  in their middle points in length. In Fig. 6,  $x_0$  is the length of reinforcement distributed in concrete members, although it is not counted as a steel tie in a strut-tie model.  $T_i$ , a member force of a steel tie  $i$ , is determined by the sum of the prestressing force ( $= 0.75A_{ps}f_{pu}$ ,  $A_{ps}$  = cross-sectional area of prestressing strands,  $f_{pu}$  = tensile strength of prestressing strands) of strands at the location of the steel tie  $i$ , the member force of the steel tie  $i$  in a strut-tie model subjected to the prestressing force acting passively on the concrete member (as shown in Fig. 8(a)), and the tensile member force of the steel tie in a strut-tie model subjected to external vertical load.

### 3. Application of nonlinear strut-tie model approach

#### 3.1. Summary of shear test results

The validity of the nonlinear strut-tie model approach for pre-tensioned concrete deep beams is

Table 1 Information of pre-tensioned concrete deep beams

(a) Concrete

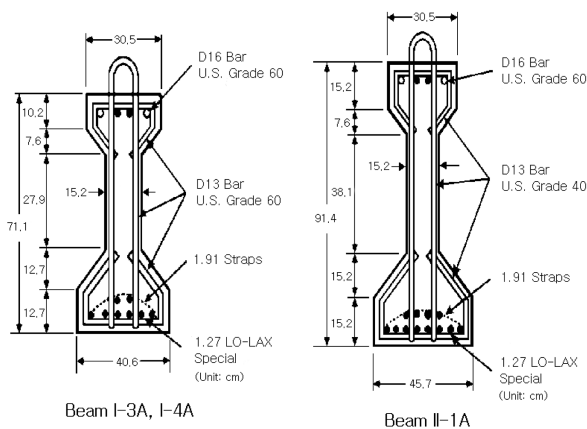
Beams		Type I-4A		Type I-3A		Type II-1A	
Prestress	Transfer	Test	Transfer	Test	Transfer	Test	
$f'_c$ (MPa)	40.27	60.74	40.27	60.74	41.23	61.71	
$E_c$ (GPa)	38.75	39.51	38.75	39.51	38.47	40.68	
$f_r$ (MPa)	6.34	-	6.34	-	6.34	-	

(b) Prestressing strand (Grade 270)

Beams		Type I-4A		Type I-3A		Type II-1A	
Strand Location	Top	Bottom	Top	Bottom	Top	Bottom	
$A_{ps}$ (cm <sup>2</sup> )	1.05	1.05	1.05	1.05	1.05	1.05	
$d_p'$ , $d_p$ (cm)	5.08	66.00	5.08	64.77	5.08	84.66	
$E_{ps}$ (GPa)	192.5	192.5	192.5	192.5	192.5	192.5	
$f_{pu}$ (MPa)	1.94	1.94	1.94	1.94	1.94	1.94	
$f_{sf}$ (MPa)	1.43	1.33	1.43	1.33	1.43	1.33	
$f_{se}$ (MPa)	1.39	1.27	1.39	1.27	1.39	1.27	
$P_e$ (kN)	290.6	1092.0	291.9	1073.3	291.9	1599.8	

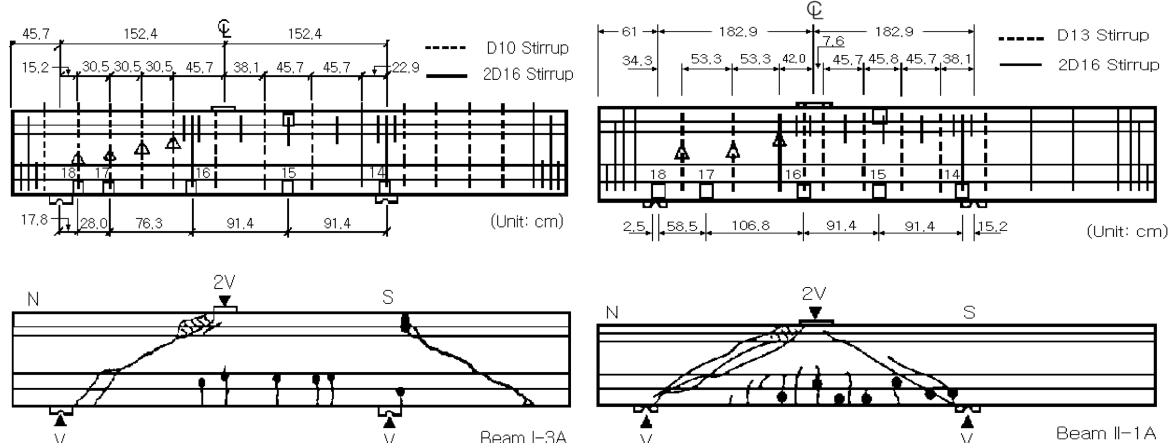
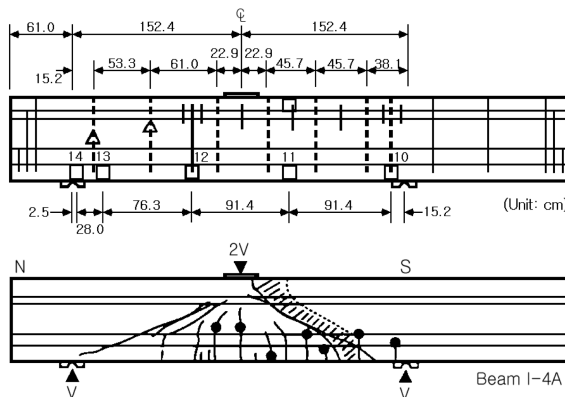
(c) Mild reinforcement

Beams		Type I-4A		Type I-3A		Type II-1A	
Reinforcement	D16	D13	D16	D10	D16	D13	
U.S. Grade	60	40	60	40	60	40	
$A_s$ ', $A_v$ (cm <sup>2</sup> )	2.00	1.23	2.00	0.67	1.87	1.23	
$E_s$ (GPa)	200.1	203.4	200.1	201.0	197.0	203.4	
$f_y$ (MPa)	441.3	358.5	441.3	317.2	427.5	358.5	



(a) Cross Sections

--- D13 Stirrup  
— 2D16 Stirrup



(b) Details and Failure Crack Patterns

Fig. 7 Test specimens of pre-tensioned concrete beams

examined by evaluating the behavior and strength of I-typed three pre-tensioned concrete deep beams tested to failure at Purdue University (Kaufman 1989). The specimens were full scale pre-tensioned AASHTO Type I and II beams with span-to-depth ratios of 4.0 and 4.3. The beam dimensions, reinforcement details, crack patterns at failure, and strain gage locations are shown in Fig. 7. The strain gages were attached to the prestressing strands and mild reinforcements. Before placing the strain gages, the prestressing strands were tensioned to 22.2 kN. Following instrumentation, the prestressing strands were stressed to  $150.4 \text{ kN} = 0.75A_{ps}f_{pu}$ . Detailed specimen information is given in Table 1.

In Beam I-4A, the first diagonal crack opened in the *S*-shear span at a shear of 524.9 kN. This was followed by a diagonal crack in the *N*-shear span at a shear of 533.8 kN. Failure started with an initial spalling of the concrete under the edge of the loaded plate in the *S*-shear span, followed by web crushing at a shear force of 718.4 kN. The failure zone is identified by the shaded region in Fig. 7(a). A yielding of the stirrup reinforcement was observed upon the formation of the inclined shear crack. The strain measurements for the strands indicated no bond deterioration as the shear force approached failure level.

In Beam I-3A, flexural cracking was first observed, followed by a web-shear crack in the *N*-shear span. About half of the prestressing strands showed some slip upon formation of the web-shear crack. A major inclined crack developed at a shear of 435.9 kN. The instrumented prestressing strands near the support of the *N*-side of the beam showed a drop in the strain level upon inclined shear cracking. Failure was initiated by extensive slip of all strands on the *N*-side, followed by crushing of the concrete near the loading plate on the same shear span at a shear of 502.9 kN.

In Beam II-1A, major inclined shear cracks developed first in the *S*-shear span at a shear force of 667.2 kN. This was followed by a second web-shear crack in the *N*-shear span at a shear force of 702.8 kN. Failure followed initial spalling of the concrete near the edge of the bearing plate at a shear force of 987.9 kN. This was followed by crushing of the top flange concrete in the *N*-shear span. The strain measurements for the strands near the support indicated some bond deterioration as the shear force was 97% of the failure load.

### 3.2. Applications

To select a strut-tie model for Beam I-4A, the compressive principal stress trajectories were obtained by conducting a plain plane concrete finite element nonlinear analysis in which the hypoelastic incremental stress-strain constitutive model, the smeared cracking model, and the tension stress-strain fracture model were employed. Fig. 8 shows the compressive principal stress trajectories at loading steps 1 and 2 respectively. The stress trajectories indicated that the concentrated loads at loading steps 1 and 2 were carried mainly in the middle of the beam between the two supports. Accordingly, a strut-tie model was selected for that specific region only. The stress trajectories indicated that two major struts running from the applied load to the supports were required. A set of struts was also deemed necessary to approximate the flow of the compressive principal stresses in the upper flange. The prestressing strands were represented by the horizontal ties at the centroid of the prestressing strands, and vertical ties were placed at each stirrup location within the shear span. The selected strut-tie model is shown in Fig. 9(a). The strut-tie models for Beams I-3A and II-1A, as shown in Figs. 9(b) and 9(c), respectively, were selected similarly.

Additionally, to consider the effect of aggregate interlock action in the strut-tie model analysis of the three pre-tensioned concrete deep beams, the aggregate interlock struts 38 and 39 at the

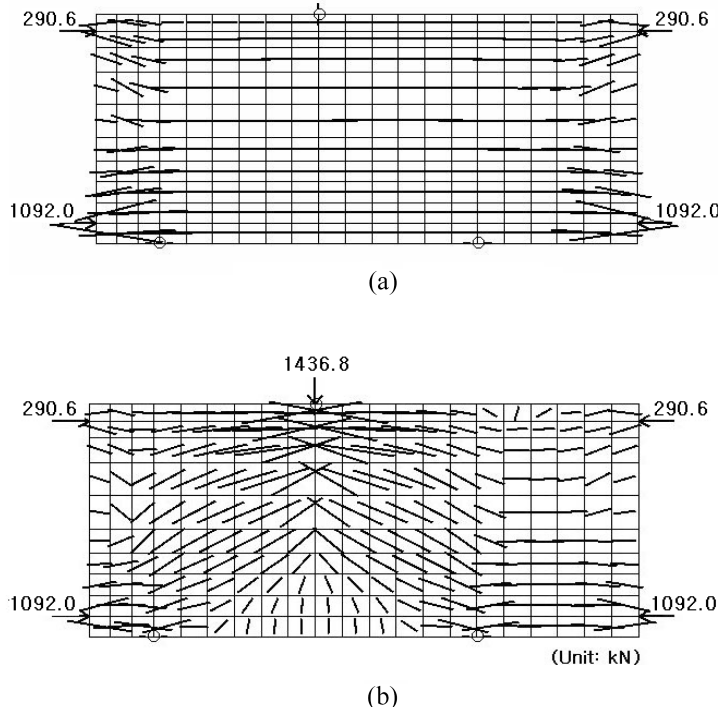


Fig. 8 Compressive principal stress flows of Beam I-4A: (a) Loading step 1; (b) Loading step 2

locations of the diagonal concrete struts 36 and 37 respectively in the Beam I-4A strut-tie model and the aggregate interlock struts 42 and 43 at the locations of the diagonal concrete struts 40 and 41 respectively in the Beam I-3A and II-1A strut-tie models were additionally placed. In addition, to consider the effect of tensile capacity of concrete ties, three cases were considered in current study: no concrete ties, horizontal concrete ties at the location of prestressing strands, and horizontal concrete ties and vertical concrete ties at the locations of prestressing strands and vertical stirrups, respectively.

The prestressing forces for the three pre-tensioned concrete deep beams were applied to the corresponding nodes of the beam strut-tie models by using the concept of gradual introduction of prestressing force introduced previously. The transfer lengths of the prestressing forces in Beam I-4A, I-3A, and II-1A were calculated as 79.5, 78.2, and 77.7 cm respectively. Since the three deep beams have sufficient transfer length in their S-shear spans, all effective prestressing forces were applied to the first nodes of the beam strut-tie models. In the N-shear spans, the effective prestressing forces were distributed to the nodes of the strut-tie models located within the transfer lengths by using linear interpolation. Additionally, for comparison of imposing methods of the prestressing force in Beam I-4A, the effective prestressing force was applied to the most fringed node of the Beam I-4A strut-tie model as concentrated force. The effective prestressing forces imposed to the strut-tie models are shown in Fig. 9.

The effective strengths of all concrete struts in the beam strut-tie models were initially determined using Yun and Ramirez's (1996) procedure, in which the principal stress ratios of the finite elements modeling the struts and the deviation angles between the struts and compressive principal stress

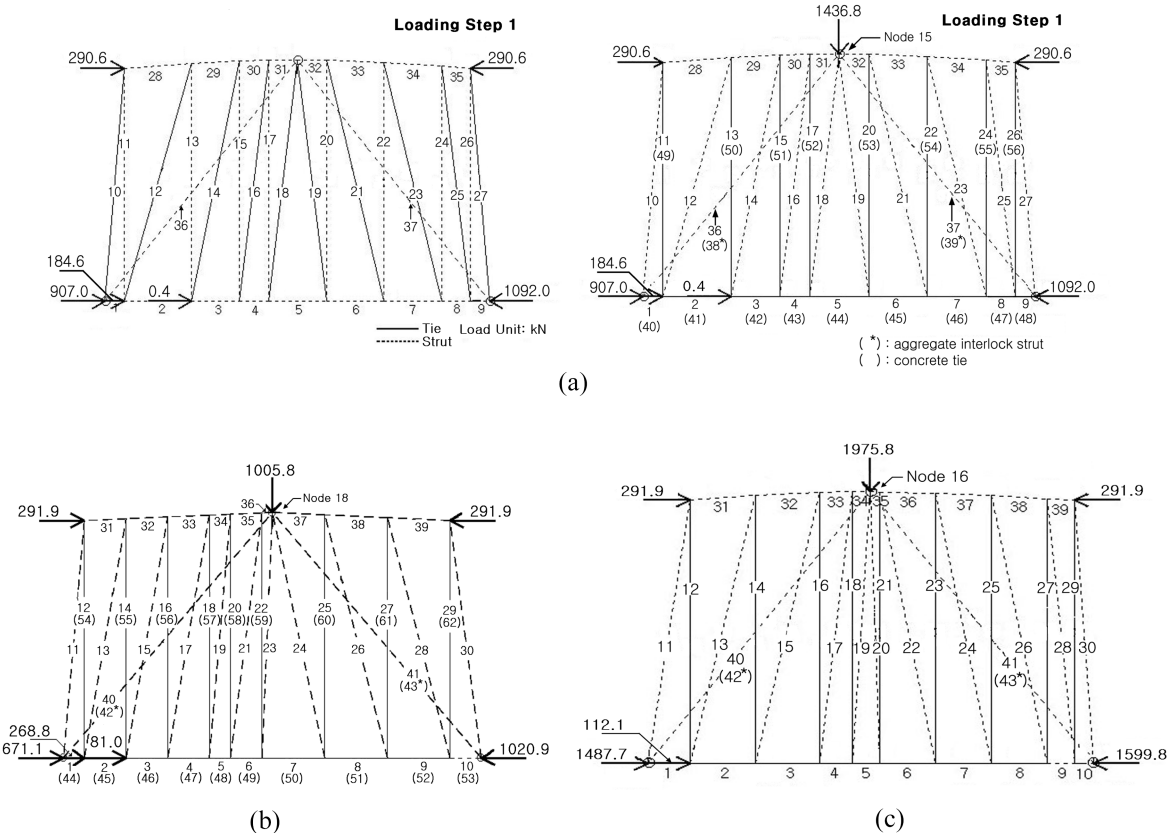


Fig. 9 Strut-tie models: (a) Beam I-4A; (b) Beam I-3A; (c) Beam II-1A

trajectories were implemented, and then later modified using the procedure proposed by Yun (2005), in which the degree of confinement in relation to reinforcement details was considered. Since the confining forces of tensile reinforcing bars and prestressing strands act passively on the beams, the effective strengths of concrete struts located at confining regions increase. The effective strengths of the aggregate interlock struts were taken as the uniaxial compressive strength of the concrete. The effective strengths of concrete ties and steel ties were taken as the tensile strength of the concrete and the yield strength of the steel respectively. Table 2 lists the effective strengths of concrete struts in the beam strut-tie models subjected to their failure loads.

The cross-sectional area of a concrete strut,  $A_{strut}$ , and a steel tie,  $A_{tie}$ , in a selected strut-tie model were determined using Yun's (2000) algorithm that requires only a few iterations within the effective strength limits to satisfy the following conditions.

$$P_{rs} \leq \phi_s A_{strut} f_s \quad (8a)$$

$$P_{rt} \leq \phi_t A_{tie} f_t \quad (8b)$$

where  $P_{rs}$  and  $P_{rt}$  are respectively the design forces of the strut and tie,  $f_s$  and  $f_t$  are respectively the

Table 2 Effective strengths of concrete struts

Beams	Strut No.	Strut No.	Strut No.	Strut No.
I-4A	10	0.61	21	0.19
	12	0.37	23	0.52
	14	0.22	25	0.44
	16	0.19	27	0.61
	18-19	0.20	28	0.88
I-3A	10	1.00	21,23	0.20
	11	0.66	24	0.16
	13	0.27	26	0.29
	15	0.19	28	0.33
	17	0.31	30,37,38	0.67
	19	0.22	31,32,36	1.00
II-1A	9	0.66	19,20,24	0.20
	10	1.00	26	0.26
	11	0.61	28	0.24
	13	0.41	30	0.56
	15	0.22	31,32,34	1.00
	17,22	0.17	33	0.60

See Fig. 9 for strut numbers; \*: aggregate interlock strut

Table 3 Cross-sectional areas of concrete struts

Beams	Strut No.	Areas (cm <sup>2</sup> )	Strut No.	Areas (cm <sup>2</sup> )	Strut No.	Areas (cm <sup>2</sup> )
I-4A	10	115.8	23	133.7	32	166.5
	12	238.9	25	135.2	33	191.9
	14	366.3	27	96.6	34	83.6
	16	370.3	28	73.9	35	69.8
	18	327.1	29	178.3	36	356.0
	19	324.5	30	193.7	37	358.9
	21	371.8	31	195.7	38*-39*	51.6
I-3A	10	22.9	26	114.7	37	151.2
	11	29.7	28	103.2	38	120.3
	13	117.1	30	62.2	39	66.0
	15	165.3	31	55.4	40	332.8
	17	100.1	32	69.6	41	370.3
	19	126.8	33	118.1	42*	12.9
	21	291.4	34	137.6	43*	3.22
	23	273.5	35	153.4	-	-
	24	191.7	36	114.3	-	-
II-1A	9	12.6	24	296.6	36	307.9
	10	12.6	26	238.3	37	104.1
	11	113.2	28	238.3	38	73.7
	13	179.0	30	101.9	39	58.0
	15	337.8	31	74.5	40	707.3
	17	65.3	32	114.6	41	661.2
	19	322.3	33	257.3	42*	38.7
	20	269.7	34	174.9	43*	32.3
	22	368.4	35	165.5	-	-

See Fig. 9 for strut numbers; \*: aggregate interlock strut

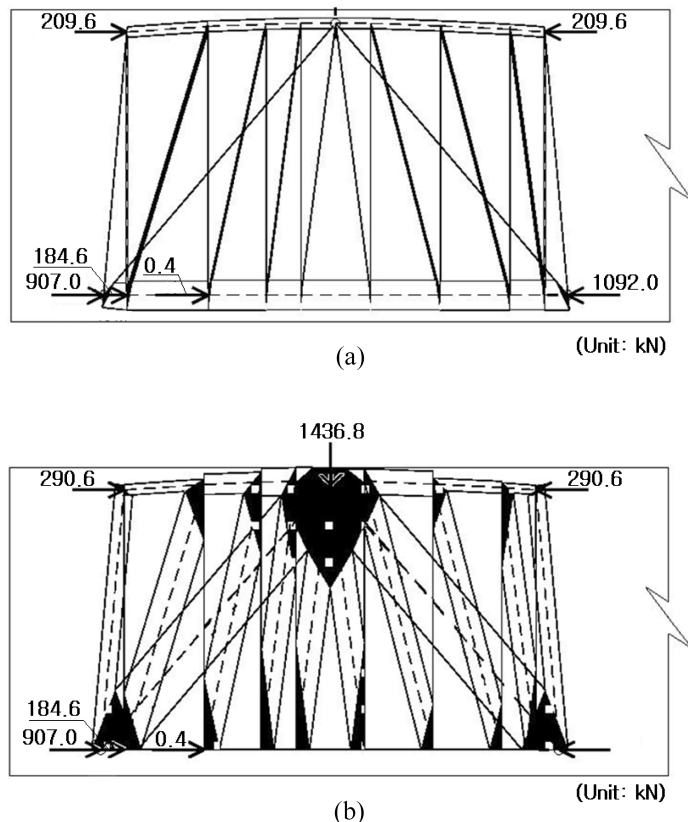


Fig. 10 Dimensioned strut-tie model for Beam I-4A: (a) Loading step 1; (b) Loading step 2

effective strengths of the strut and tie, and  $\phi_s$  and  $\phi_t$  are respectively the strength reduction factors of the strut and tie which are equal to 1 in the strut-tie model analysis of concrete members. Table 3 lists the cross-sectional areas of concrete struts in the beam strut-tie models subjected to their failure loads. The cross-sectional areas of steel ties at the locations of the vertical stirrups and horizontal prestressing strands determined from Eq. (8) were set as the areas of the vertical stirrups and horizontal prestressing strands in the analyses of the strut-tie model themselves. The cross-sectional areas of the aggregate interlock struts 38 and 39 in the Beam I-4A strut-tie model, determined by equating the strut force obtained from the structural analysis of the strut-tie model to the frictional force obtained by using the vertical steel tie forces of the strut-tie model, were determined as  $51.6 \text{ cm}^2$ . The cross-sectional areas of the aggregate interlock struts 42 and 43 in the Beam I-3A and II-1A strut-tie models were determined to be as  $12.9 \text{ cm}^2$  and  $3.2 \text{ cm}^2$  respectively. The cross-sectional areas of the concrete ties ( $169.1 \text{ cm}^2$  and  $182.6 \text{ cm}^2$  respectively for the horizontal concrete ties 40-48 and the vertical concrete ties 49-56 in the Beam I-4A strut-tie model,  $182.6 \text{ cm}^2$  for the horizontal concrete ties 54-62 in the Beam I-3A and II-1A strut-tie models, and  $162.1 \text{ cm}^2$  and  $230 \text{ cm}^2$  for the vertical concrete ties 44-53 respectively in the Beam I-3A and II-1A strut-tie models) placed additionally at the location of steel ties were taken from the circular concrete areas around the reinforcing bars that do not overlap each other, as shown in Fig. 5. The dimensioned strut-tie model for Beam I-4A, as shown in Fig. 10, exhibited suitable geometrical configurations, which fit

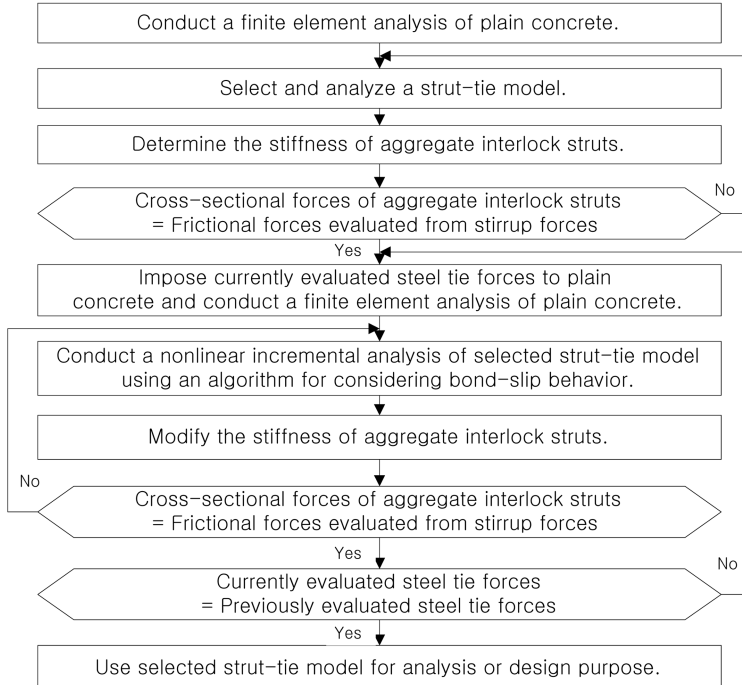


Fig. 11 Algorithm of nonlinear strut-tie model approach implemented with effects of aggregate interlock, concrete confinement by reinforcement, and bond slip of prestressing strands

the sizes of the beams and prevented any overlapping struts placed almost parallel. Dimensioned strut-tie models for the other beams also exhibited suitable geometrical configurations.

The failure strengths of the three pre-tensioned concrete deep beams tested to failure were evaluated using the method proposed by Yun (2000), in which the criteria for the ultimate limit state were: (a) the occurrence of a nodal zone failure mechanism, (b) the instability of the selected strut-tie model due to the strength reduction of struts and ties during incremental loading steps, and (c) the violation of the strut-tie model's geometric compatibility condition. In addition, the structural behavior of the deep beams was evaluated by conducting a finite element material nonlinear analysis of the selected strut-tie models. Fig. 11 shows the strut-tie model analysis and design algorithm that considers the effects of aggregate interlock struts, concrete confinement by steel ties, and bond slip of prestressing strands in the nonlinear strut-tie model approach.

### 3.3. Evaluation of strut-tie model analysis results

#### 3.3.1. Beam I-4A and Beam II-1A without consideration of bond slip effect

Since the cross-sectional areas of the struts and ties in the selected strut-tie models were decided, the finite element material nonlinear analyses of the strut-tie model themselves were conducted to identify the strain behaviors and evaluate the strengths of the deep beams by checking the stability of the selected strut-tie models. Fig. 12 compares the strand forces of Beam I-4A and II-1A obtained from experiments and strut-tie model analyses. In the figures, 'Case 0' is the results

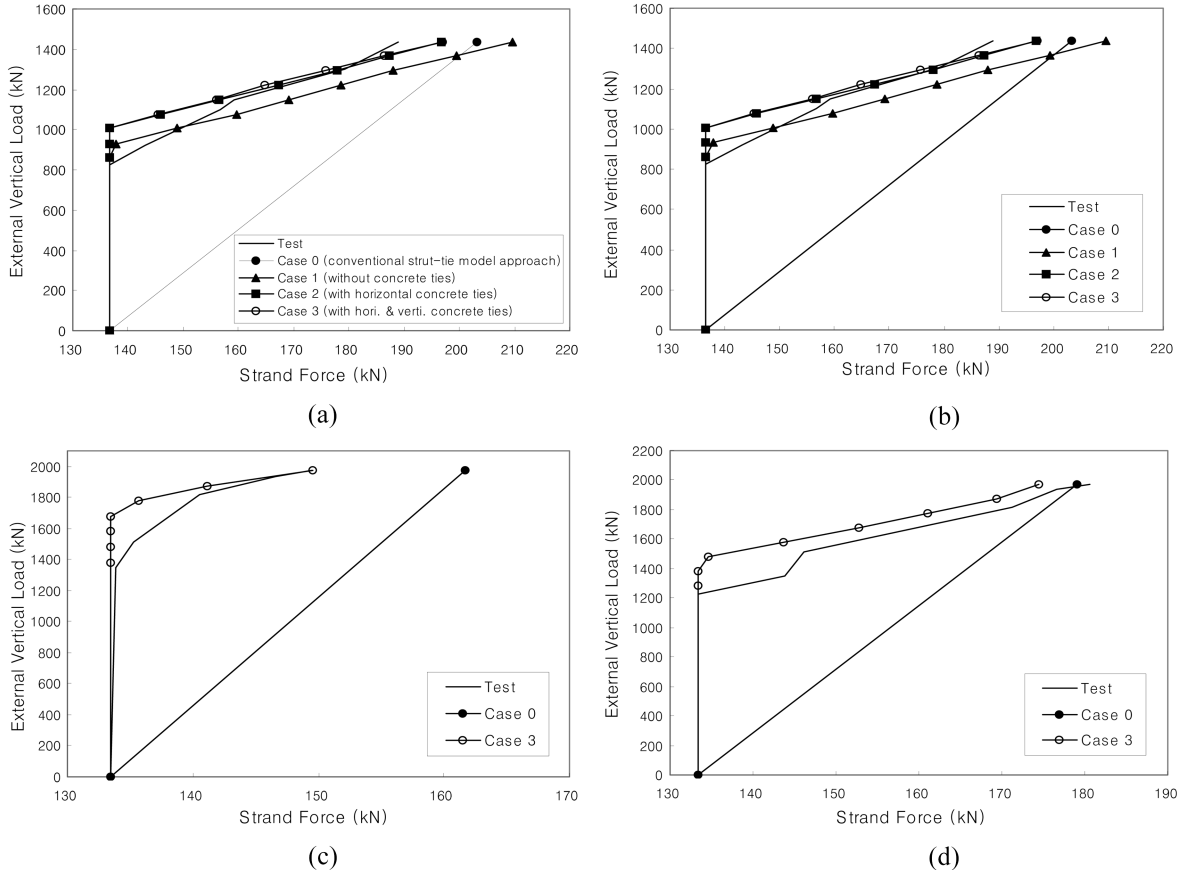


Fig. 12 Longitudinal strand forces: (a) Gage 11, Beam I-4A; (b) Gage 13, Beam I-4A; (c) Gage 14, Beam II-1A; (d) Gage 16, Beam II-1A

obtained by applying the conventional linear strut-tie model approach in which additional concrete ties and nonlinear techniques are not incorporated into the strut-tie model analysis and design. ‘Case 1’, ‘Case 2’, and ‘Case 3’ are the results obtained by applying the nonlinear strut-tie model approach with no concrete ties, the horizontal concrete ties only at the location of prestressing strands, and the horizontal concrete ties at the location of prestressing strands and the vertical concrete ties at the locations of vertical stirrups, respectively. The figure shows that the analytical results obtained from the nonlinear strut-tie model approach are closer to the experimental results than those obtained from the conventional linear strut-tie model approach. Additionally, when both the vertical and horizontal concrete ties were considered, the mid-span deflections of the deep beams were closer to actual deflections as shown in Fig. 13.

The cross-sectional areas and forces of the aggregate interlock struts were determined to satisfy Eq. (4) when these struts failed. The reason to take the cross-sectional forces when the struts failed is that there will be no more aggregate interlock due to the increase of crack width when the tensile strains of the vertical stirrups are large. Fig. 14 shows the variation of the cross-sectional forces of the aggregate interlock struts in terms of the increase of external vertical load at Beam I-4A, and

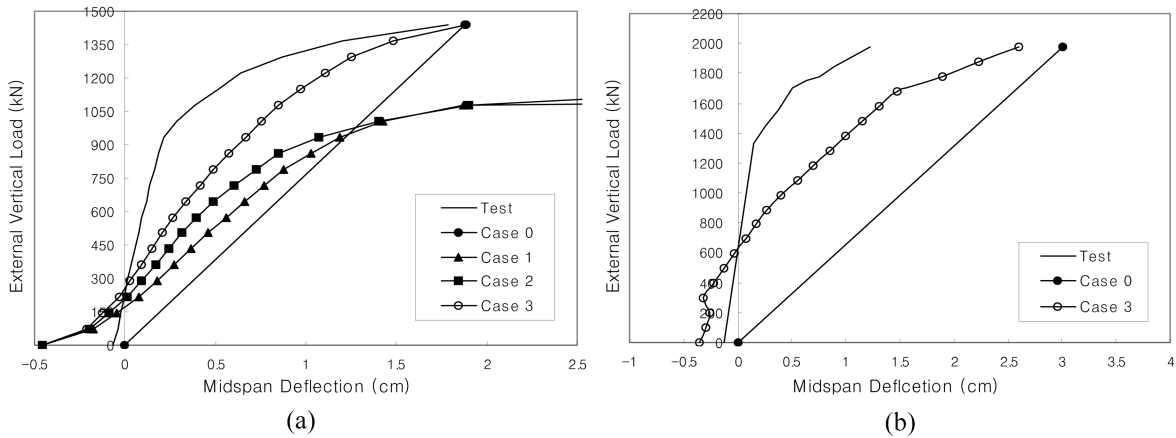


Fig. 13 Mid-span deflection: (a) Beam I-4A; (b) Beam II-1A

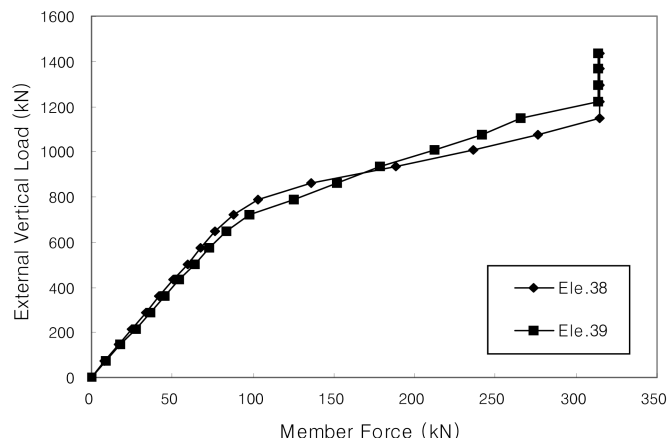


Fig. 14 Variation of aggregate interlock member forces of Beam I-4A

shows that the aggregate interlock struts failed before the failure loads were applied. Fig. 15 compares the strand forces of Beam I-4A obtained from the experiment and the strut-tie model analysis with/without consideration of the aggregate interlock struts. In the case of no aggregate interlock struts the strand force is smaller than the experimental result. This is because there is no direct transfer of the external vertical load to the supports through the aggregate interlock. Thus, the aggregate interlock behavior must be considered in the analysis and design of pre-tensioned concrete beams.

Fig. 16 illustrates the effect of imposing methods of the external prestressing force to the strut-tie model for Beam I-4A. Dispersing the prestressing force at the strut-tie model nodes within the transfer length allowed us to trace the variation of the prestressing strand force better than concentrating the prestressing force. In addition, the vertical ties 11, 12, and 15 at the locations of the vertical stirrups have large cross-sectional forces in the case of dispersing the prestressing forces in the ultimate state, indicating that the imposing methods of the external prestressing force to a

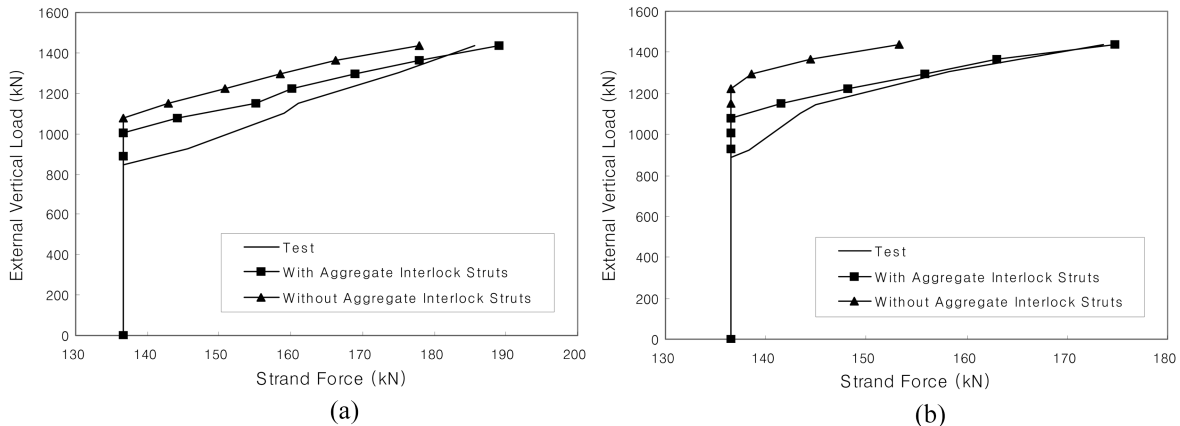


Fig. 15 Effect of aggregate interlock on longitudinal strand force of Beam I-4A: (a) Gage 12; (b) Gage 13

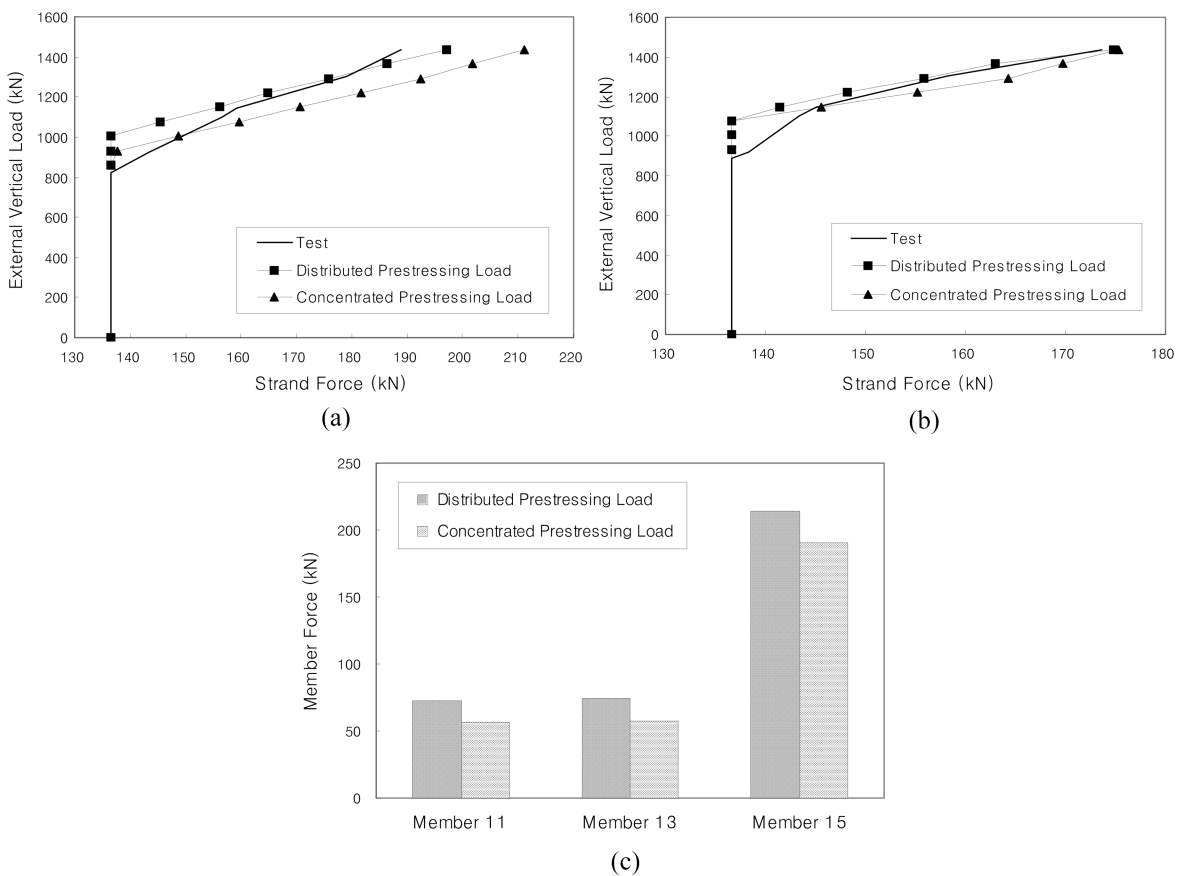
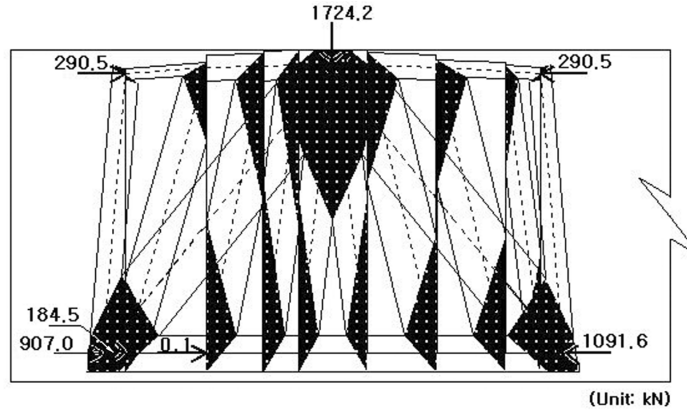
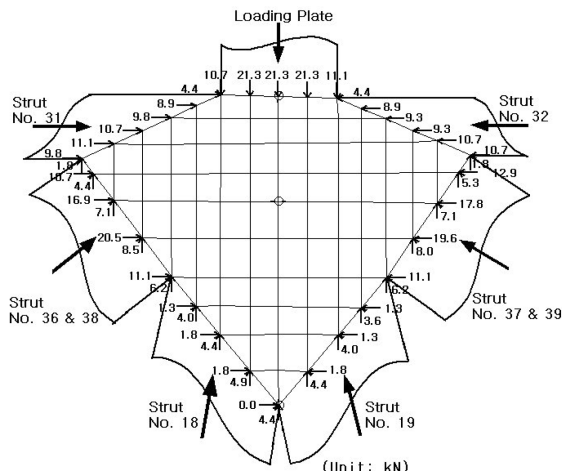


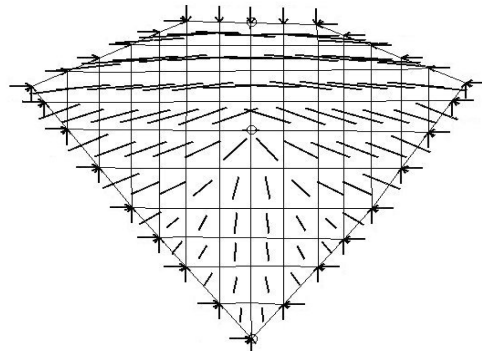
Fig. 16 Longitudinal strand and vertical stirrup forces of Beam I-4a according to different application types of prestressing force: (a) Strand Force at Gage 11; (b) Strand Force at Gage 13; (c) Stirrup Forces



(a) Dimensioned Strut-Tie Model under 120% Failure Load



(b) Finite Element Model



(c) Compressive Principal Stress Flow

Fig. 17 Strength verification of critical nodal zone in Beam I-4a strut-tie model (without bond slip effect)

strut-tie model can affect the results of shear design. Therefore, in the strut-tie model analysis and design of pre-tensioned concrete beams it is judged that the prestressing force must be introduced gradually to the strut-tie model nodes located within the transfer length.

The strength of the nodal zone shaped by the loading plate, corresponding to the node 15 of the Beam I-4A strut-tie model in Fig. 9, was evaluated using a plane plain concrete finite element nonlinear analysis. The configuration of the nodal zone was determined based on the dimensioned strut-tie model that could carry the maximum load in a stable status. The maximum load that the Beam I-4A strut-tie model could carry was 120% of the experimental failure load. Fig. 17(a) illustrates the dimensioned strut-tie model under the maximum load. Figs. 17(b) through 17(g) illustrate the finite element model for the nodal zone, the compressive principal stress flow, and the cracking and crushing shapes according to load levels. In Fig. 17(b), after a finite element grid was

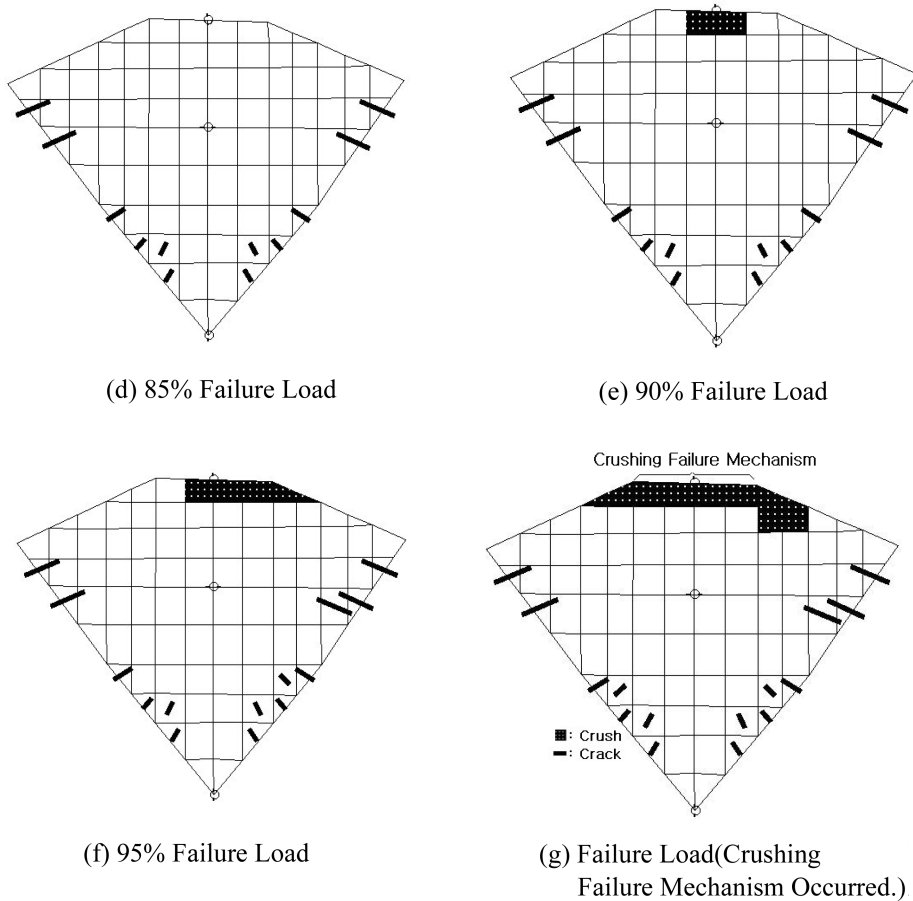


Fig. 17 Continued

laid out in the nodal zone, the axial forces in the individual struts and the loading plate were divided into their components and applied as concentrated loads at the corresponding nodes of the finite elements. The compressive principal stress flow of the nodal zone, as shown in Fig. 17(c), is similar to that of Fig. 8(b). When the experimental failure load was applied, a crushing failure mechanism occurred under the loading plate, although it was not the same as the failure shape shown in Fig. 7(a). This indicates that the nonlinear strut-tie model accurately predicted the failure strength of Beam I-4A by examining the condition of the occurrence of a nodal zone failure mechanism. Here, a failure mechanism is assumed to occur when cracks propagate from one side to the opposite side of the nodal zone and/or when all boundary elements along any nodal zone face crush, following the proposal by Yun (2000). The locations and angles of the cracks on the lower side area of the nodal zone are very similar to the ones that occurred in the experiment. The maximum compressive principal stress in the nodal zone when the failure mechanism occurred was  $1.18f_c'$ . The strength of the nodal zone corresponding to the node 16 of the Beam II-1A strut-tie model in Fig. 9 was also verified in the current study. The geometry of the nodal zone was determined based on the dimensioned strut-tie model that could carry the maximum load in a stable

status. When the experimental failure load was applied, a crushing failure mechanism occurred under the loading plate. The maximum compressive principal stress in the nodal zone when the failure mechanism occurred was  $1.17f_c'$ .

### 3.3.2. Beam I-3A and Beam II-1A with consideration of bond slip effect

The algorithm that considers the effect of bond slip of prestressing strands on the behavior and strength of pre-tensioned concrete beams was developed and implemented to the nonlinear strut-tie model approach (Yun 2000). And, the validity of the algorithm is verified through the behavior and strength evaluations of Beam I-3A and II-1A in which the bond slip occurred. Since the strut-tie models that included the horizontal and vertical concrete ties evaluated the experimental results more accurately than those that did not include, the horizontal and vertical concrete ties were included in Beam I-3A and II-1A strut-tie models.

In the nonlinear strut-tie model approach employed in the current study, it was assumed that the tensile force of a prestressing strand tie after bond slip has been transferred to the concrete tie that was additionally placed at the location of the prestressing strand tie. Since Eq. (5) is the average bond stress equation for a deformed bar, the average bond stress equation for prestressing strands is required. In current study, the equation for a deformed bar as the one for prestressing strands was used by multiplying a reduction factor 0.67. The reduction factor was obtained by dividing the bond stress  $\mu$  of the prestressing strand tie located at the left lowest part of Beam I-3A strut-tie model at the incremental load step in which the bond slip occurred in the experiment, by the average bond stress  $\mu_{avg}$  of the prestressing strand tie. The same reduction factor was also used to estimate the average bond stress in the strut-tie model analysis of Beam II-1A.

The values of  $\Delta T$  obtained by Eq. (7) in the nonlinear finite element analyses of the selected strut-tie model themselves are shown in Table 4 with the predicted locations and incremental load steps in which the bond slip occurred. The predicted locations are identical to those recorded in the experiments. In Beam I-3A and II-1A, it was predicted that the bond slip occurred at 85% and 95% of the experimental failure loads of the deep beams, respectively. The predicted loads are similar to the measured loads, i.e., 87% and 97% of the experimental failure loads of the deep beams. This result indicates that the nonlinear strut-tie model approach incorporating the algorithm for the bond slip behavior in pre-tensioned concrete members can accurately estimate the location of bond slip

Table 4 Difference of cross-sectional force,  $\Delta T$ , between steel ties

Beams	Incremental Loading Step	Steel Tie No.			
		1**	2	3	4
I-3A	17*	134.3	90.8	6.6	0
	18	136.2	106.2	6.6	0
	19	136.2	106.2	6.6	0
	20	139.8	111.0	8.5	7.6
II-1A	17	279.9	0	71.8	35.5
	18	290.8	0	83.5	37.4
	19*	302.5	4.6	93.9	42.7
	20	317.7	90.6	104.6	48.0

Units for  $\Delta T$  = kN; See Fig. 9 for steel tie numbers; \*: Incremental loading step that bond slip occurs first; \*\*: steel tie which experiences bond slip

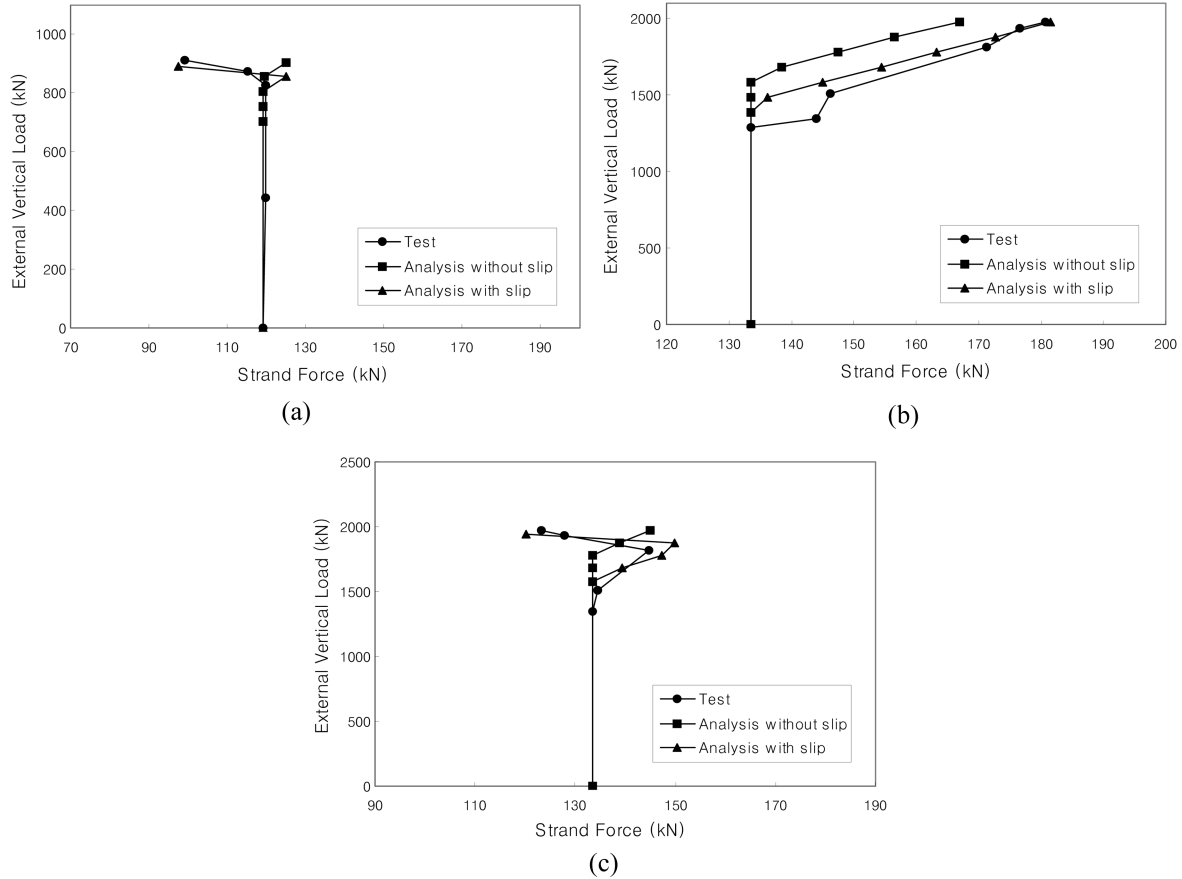


Fig. 18 Longitudinal strand forces: (a) Gage 18, Beam I-3A; (b) Gage 16, Beam II-1A; (c) Gage 18, Beam II-1A

and magnitude of external vertical load inducing the bond slip of prestressing strands. Fig. 18 compares the internal forces of prestressing strands of Beam I-3A and II-1A measured in the experiments with the internal forces obtained by the nonlinear strut-tie model approach. It shows that the nonlinear strut-tie model approach that included the algorithm for bond slip behavior estimates the internal forces relatively close to the experimental results compared with the approach that did not include the algorithm.

Since the concrete crushing near the loading plate in Beam I-3A occurred when the deep beam failed, the bearing capacity of the nodal zone under the loading plate in the Beam I-3A strut-tie model was verified. Fig. 19 illustrates the configuration of the nodal zone, the compressive principal stress flows, and the cracked and crushed shapes according to load levels. The directions of the compressive principal stress flows were close to those of the corresponding region. When the experimental failure load of Beam I-3A was applied, a crushing failure mechanism at the nodal zone boundary constructed by the loading plate occurred, indicating that the failure strength of the deep beam was exactly estimated by the condition of nodal zone strength among the three ultimate limit state conditions defined previously. The cracked and crushed shape of the nodal zone was

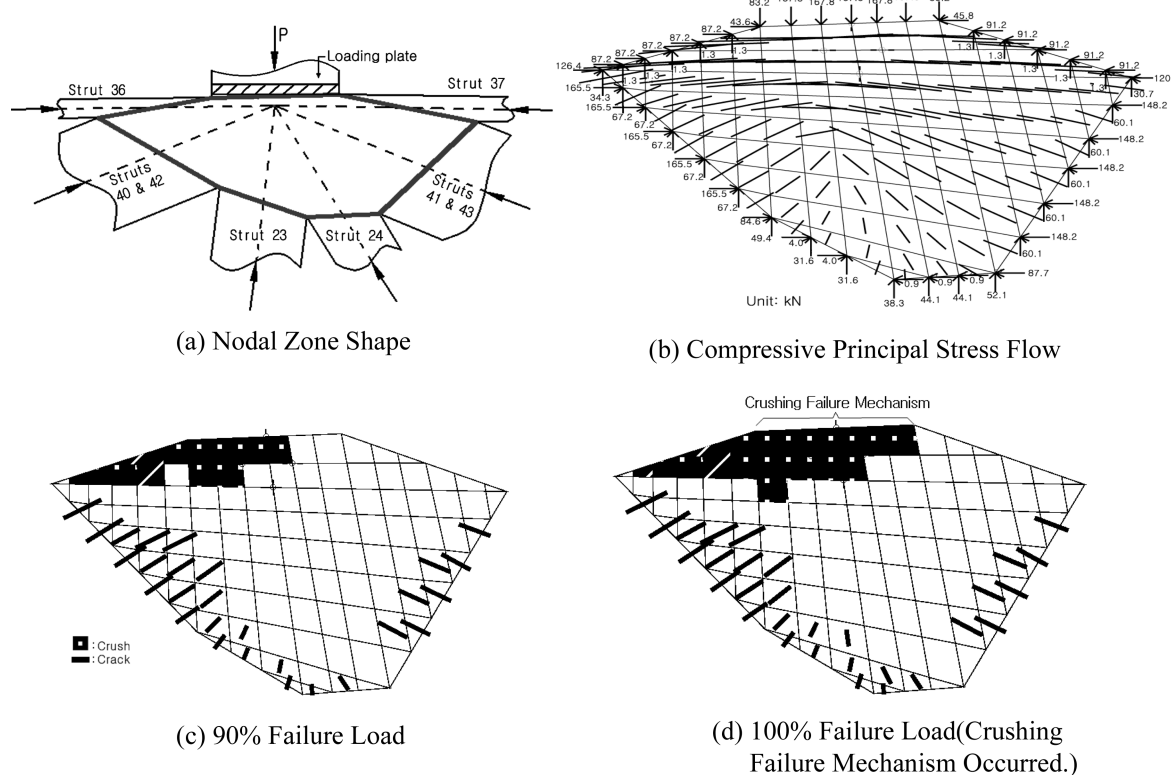


Fig. 19 Strength verification of critical nodal zone in Beam I-3A strut-tie model

similar to the shapes in the experiment. The maximum compressive principal stress at the nodal zone when the crushing failure mechanism occurred was  $1.09f'_c$ .

The bearing capacity of the nodal zone under the loading plate in the Beam II-1A strut-tie model that included the effect of bond slip behavior was also verified. Fig. 20 illustrates the configuration of the nodal zone, the compressive principal stress flows, and the cracked and crushed shapes according to load levels. The directions of the compressive principal stress flows were close to those of the corresponding region of the plain plane concrete finite element analysis model. When 90% of the experimental failure load of Beam II-1A was applied, a crushing failure mechanism at the nodal zone boundary constructed by the loading plate occurred, indicating that the failure strength of the deep beam was well estimated by the condition of nodal zone strength. The cracked and crushed shape of the nodal zone was similar to the shapes in the experiment. The maximum compressive principal stress at the nodal zone when the crushing failure mechanism occurred was  $1.25f'_c$ .

The failure strengths of the three pre-tensioned concrete deep beams were predicted by the nonlinear strut-tie model approach employing the three ultimate limit state criteria defined previously, the ACI 318-02 (2002), the modified compressive field theory (Vecchio and Collins 1986), and the modified sectional truss model (Ramirez and Breen 1983). The results are presented in Table 5.

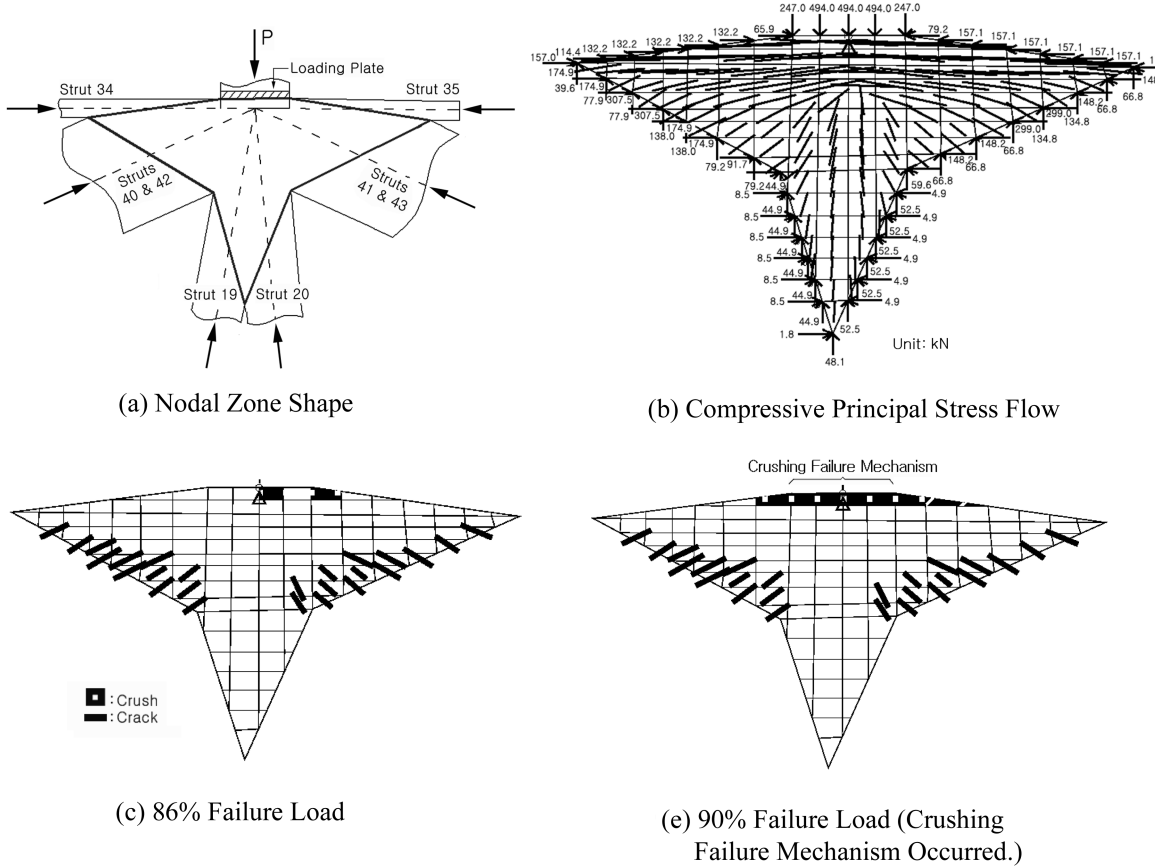


Fig. 20 Strength verification of critical nodal zone in Beam II-1a strut-tie model (with bond slip effect)

Table 5 Shear strength of pre-tensioned concrete deep beams

Beams	$V_{test}$ (kN)	$V_{evaluated} / V_{test}$			
		ACI 318-02	MCFT	MSTM	Current Study
I-4A	718.4	0.70	0.70	0.74	1.00
I-3A	502.9	0.85	0.97	0.78	1.00*
II-1A	987.9	0.61	0.58	0.61	0.90*

MCFT: Modified Compression Field Theory; MSTM: Modified Sectional Truss Model; \*: Shear strength obtained by consideration of bond slip

#### 4. Conclusions

In this study, the validity of the nonlinear strut-tie model approach for the analysis and design of pre-tensioned concrete deep beams was examined through the behavior and strength analysis of pre-tensioned concrete deep beams tested to failure. Based on the analytical results, the following conclusions are obtained:

1. In a prestressed concrete beam, the prestressing force enhances the behavior and strength of the

beam by increasing the aggregate interlock resistance until large shear cracks occur. Therefore, in the strut-tie model analysis and design of prestressed concrete beams, the effect of the aggregate interlock must be considered by a method such as the one presented in current study. In addition, applying the non-linear strut-tie model approach to the analysis of pre-tensioned concrete deep beams, in which the prestressing force considered as the external load was applied to the strut-tie model nodes located within the transfer length of prestressing strands, predicted the structural behavior more accurately. Therefore, it is suggested that prestressing force be introduced to a strut-tie model gradually in strut-tie model analysis and design of pre-tensioned concrete beams.

2. The non-linear strut-tie model approach implemented with the algorithm considering the effect of the bond slip of prestressing strands predicted the same locations of bond slip of prestressing strands as those recorded in the experiments, estimated the magnitude of external loads that caused the bond slip of prestressing strands in the pre-tensioned concrete deep beams in which the bond slip occurred accurately, and evaluated the failure strengths of the three pre-tensioned concrete deep beams tested to failure and the internal forces of prestressing strands very well. Therefore, it seems that the average bond strength equation of prestressing strands, the basic assumptions for the estimation of the bond stress of prestressing strands, and the tensile force equation of prestressing strands are regarded as appropriate, and the nonlinear strut-tie model approach presented in current study was proven to be a viable method for the analysis of pre-tensioned concrete deep beams. Accordingly, the nonlinear strut-tie model approach, with the capability of predicting the anchorage failure of prestressing strands, can be effectively used in the analysis and design of general pre-tensioned concrete beams requiring gradual decrease of prestressing forces along beam spans.

## References

- Alshegeir, A. and Ramirez, J. A. (1992), "Strut-tie approach in pretensioned deep beams", *ACI Struct. J.*, **89**(3), 296-304.
- American Association of State Highway Transportation Officials (1998), *AASHTO LRFD BRIDGE DESIGN SPECIFICATIONS*, SI Units, 2nd Edition, Washington D.C.
- American Concrete Institute (2002), *Building Code Requirements for Structural Concrete (ACI 318-02) and Commentary (318R-02)*, American Concrete Institute, Farmington Hills, Michigan.
- Chen, B. S., Hagenberger, M. J. and Breen, J. E. (2002), "Evaluation of strut-and-tie modeling applied to dapped beam with opening", *ACI Struct. J.*, **99**(4), 445-450.
- Foster, S. J., Powell, R. E. and Selim, H. S. (1996), "Performance of high-strength concrete corbels", *ACI Struct. J.*, **93**(5), 555-563.
- Foster, S. J. and Malik, A. R. (2002), "Evaluation of efficiency factor models used in strut-and-tie modeling of nonflexural members", *J. Struct. Eng., ASCE*, **128**(5), 569-577.
- Kaufman, M. K. (1989), *The Ultimate Strength and Behavior of High Strength Concrete Prestressed Composite I-Beams*, Ph.D Thesis, School of Civil Engineering, Purdue University, Indiana, 228.
- MacGregor, J. G. (1997), *Reinforced Concrete - Mechanics and Design*, 3rd Edition, Prentice-Hall, New Jersey, 939.
- Maxwell, B. S. and Breen, J. E. (2000), "Experimental evaluation of strut-and-tie model applied to deep beam with opening", *ACI Struct. J.*, **97**(1), 142-148.
- Ramirez, J. A. and Breen, J. E. (1983), *Proposed Design Procedures for Shear and Torsion in Reinforced and Prestressed Concrete*, Research Report No. 248-4F, Center for Transportation Research, The University of Texas at Austin, Austin, Texas, 254.
- Sanders, D. H. and Breen, J. E. (1997), "Post-tensioned anchorage zones with single straight concentric anchorages", *ACI Struct. J.*, **94**(2), 146-158.
- Schlaich, J., Schaefer, K. and Jennewein, M. (1987), "Towards a consistent design of structural concrete",

- Journal of the Prestressed Concrete Institute*, **32**, 74-150.
- Siao, W. B. (1993), "Strut-and-tie model for shear behavior in deep beams and pile caps failing in diagonal splitting", *ACI Struct. J.*, **90**(4), 356-363.
- Siao, W. B. (1994), "Shear strength of short reinforced concrete walls, corbels, and deep beams". *ACI Struct. J.*, **91**(2), 123-133.
- Tan, K. H., Tong, K. and Tang, C. Y. (2001), "Direct strut-and-tie model for prestressed deep beams", *J. Struct. Eng., ASCE*, **127**(9), 1076-1084.
- Vecchio, F. J. and Collins, M. P. (1986), "The modified compression field theory for reinforced concrete elements subjected to shear", *ACI J.*, **83**(2), 219-231.
- Yun, Y. M. (2000), "Nonlinear strut-tie model approach for structural concrete", *ACI Struct. J.*, **97**(4), 581-590.
- Yun, Y. M. (2000), "Computer graphics for nonlinear strut-tie model approach", *J. Comput. in Civ. Eng., ASCE*, **14**(2), 127-133.
- Yun, Y. M. and Ramirez, J. A. (1996), "Strength of struts and nodes in strut-tie model", *J. Struct. Eng., ASCE*, **122**(1), 20-29.
- Yun, Y. M. (2005), "Evaluation of ultimate strength of post-tensioned anchorage zones", *J. Advanced Concrete Technology, JCI*, **3**(1), 149-160.

CC